Biogeosciences
Discussions

Characterizing organic matter composition in small Low and High Arctic catchments using terrestrial colored dissolved organic matter (cDOM)

Caroline Coch[1,2], Bennet Juhls[3], Scott F. Lamoureux[4], Melissa Lafrenière[4], Michael Fritz[1], Birgit Heim[1], and Hugues Lantuit[1,2]

[1] Alfred-Wegener-Institute Helmholtz Centre for Polar and Marine Research, Telegrafenberg A45, 14473 Potsdam, Germany
[2] University of Potsdam, Institute of Earth and Environmental Science, Karl-Liebknecht-Straße 24/25, 14476 Potsdam, Germany
[3] Freie Universität Berlin, Institute for Space Sciences, Department of Earth Sciences, 12165 Berlin, Germany.
[4] Queen's University, Department of Geography and Planning, Mackintosh-Corry Hall, Kingston, Ontario K7L 3N6, Canada

Correspondence to: Caroline Coch (coch.caroline@gmail.com)

Abstract. Climate change is an important control of carbon cycling, particularly in the Arctic. Permafrost degradation through deeper thaw and physical disturbances result in the release of carbon dioxide and methane to the atmosphere and to an increase in riverine dissolved organic matter (DOM) fluxes. Whereas riverine DOM fluxes of the large Arctic rivers are well assessed, knowledge is limited with regard to small catchments that cover more than 40 % of the Arctic drainage basin. Here, we use absorption measurements to characterize changes in DOM quantity and quality in a Low Arctic (Herschel Island, Yukon, Canada) and a High Arctic (Cape Bounty, Melville Island, Nunavut, Canada) setting with regard to geographical differences, impacts of permafrost degradation and rainfall events. We find that DOM quantity and quality is controlled by differences in vegetation cover and soil organic carbon content. The Low Arctic site has higher SOCC and greater abundance of plant material introducing higher lignin concentrations into the aquatic system and resulting in a stronger color of DOM than in the High Arctic. There is a strong relationship between dissolved organic carbon (DOC) concentration and absorption characteristics (cDOM) for surface waters at both sites similar to the one for the great Arctic rivers. We used the optical characteristics of DOM such as cDOM absorption, Specific UltraViolet Absorbance SUVA, UltraViolet UV Slope, Slope Ratio for assessing quality changes downstream, at baseflow and stormflow conditions and in relation to permafrost disturbance. DOM in streams at both sites demonstrated optical signatures indicative of photodegradation downstream processes, even over short distances of 2000 m. It was determined that flow pathways and the connected hydrological residence time control DOM quality. Deeper flow pathways allow the export of permafrost-derived DOM, whereas shallow pathways with shorter residence times lead to the export of fresh near-surface derived DOM. Compared to the large Arctic rivers, DOM quality exported from the small catchments studied here is much fresher and therefore prone to degradation. This work shows that optical properties of DOM will be a useful tool for understanding DOM sources and quality at a pan-Arctic scale.

1 Introduction

Climate change has important impacts on carbon cycling, particularly in the Arctic. Approximately 1300 Gt of organic carbon are stored in permafrost soils in the northern hemisphere (Hugelius et al., 2014), which is 40 % more than currently circulating in the atmosphere. Thawing permafrost and deepening of the active layer leads to the mobilization of this carbon (Osterkamp,

5 2007; Woo et al., 2008), the release of carbon dioxide (CO_2) and methane (CH_4) to the atmosphere (Schaefer et al., 2014), and to an increase in riverine dissolved organic carbon (DOC) fluxes (Frey and Smith, 2005; Le Fouest et al., 2018). Associated with warming is also the development of surface (physical) disturbances such as active layer detachments or retrogressive thaw slumps (Lacelle et al., 2010; Lamoureux and Lafrenière, 2009; Lewkowicz, 2007; Ramage et al., 2018), and thermal perturbation of the subsurface (Lafrenière and Lamoureux, 2013). As these processes influence freshwater systems, they

10 ultimately have impacts on the biological production and the biogeochemistry of the Arctic Ocean. The six largest arctic rivers (Mackenzie, Yukon, Ob, Yenisey, Lena, Kolyma) drain 53 % of the Arctic Ocean drainage basin (Holmes et al., 2012) and transport huge amounts of nutrients and dissolved organic matter (DOM) into the ocean. However, there are limited flux estimates and information on DOM quality available for the remaining 47 %, which are sourced by smaller watersheds.

Terrigenous DOM is an important source of DOC originating from allochthonous (terrestrial such as soil and plants) and

15 autochthonous (in situ production) sources (Aiken, 2014). It is modified by biotic and abiotic processes during its lateral transport to the ocean (Tank et al., 2018; Vonk et al., 2015a; Vonk et al., 2015b). Yet, little is known about the transformation of DOM along short distances in small catchments. The composition and the vulnerability to transformation of riverine DOM is influenced by several factors such as soil organic matter and vegetation, sorption processes in the mineral layers, and biodegradation and photodegradation processes (Cory et al., 2014; Mann et al., 2012; Vonk et al., 2015b; Ward and Cory,

20 2015; Ward et al., 2017). Chromophoric or colored dissolved organic matter (cDOM) is a fraction of DOM, which absorbs light in the ultraviolet and visible wavelengths (Green and Blough, 1994). Optical characteristics of CDOM such as absorption coefficients and spectral slopes can serve as proxies for DOM molecular weight and aromaticity, which in turn can help to characterize the lability of DOM (Helms et al., 2008; Neff et al., 2006; Spencer et al., 2009; Striegl et al., 2005; Weishaar et al., 2003).

25 Previous studies have focused on characterizing cDOM-DOC relationships for the large Arctic rivers and shelf areas, which exhibit a strong seasonality (Spencer et al., 2008; Stedmon et al., 2011; Walker et al., 2013). This was also shown by a global synthesis (Massicotte et al., 2017a). A handful of studies have investigated cDOM-DOC relationships in smaller Arctic catchments: Dvornikov et al. (2018) examined cDOM characteristics in surface waters of the Yamal Peninsula and cDOM-DOC relationships were examined in studies of Subarctic catchments (Balcarczyk et al., 2009; Cory et al., 2015; Larouche et

30 al., 2015; O'Donnell et al., 2014) and the High Arctic (Fouché et al., 2017; Wang et al., 2018). Optical parameters have also been used to assess the impact of permafrost disturbance on stream geochemistry in Alaska (Abbott et al., 2014), NWT Canada (Littlefair et al., 2017) and Siberia (Spence et al., 2015). As most studies focused on downstream reaches, knowledge on the

spatial variability across catchments is limited. To our knowledge, no study has examined this relationship in a Low Arctic setting or attempted to resolve geographic differences between the Low and High Arctic.

Here, we study cDOM and DOC in surface waters in the Low Arctic (Herschel Island, Yukon, Canada) and the High Arctic (Cape Bounty, Melville Island, Nunavut, Canada). The aim of this study is to (1) compare the variability and relation of DOC and cDOM in High and Low Arctic surface water environments, and (2) to investigate changes in DOM composition along longitudinal stream profiles and with regard to permafrost disturbance and rainfall events. This study will contribute to assessing riverine transport from small watersheds to the coastal Arctic Ocean.

2 Study Area

This study was carried out in two Arctic locations, Herschel Island in the Low Arctic and at the Cape Bounty Arctic Watershed Observatory, Melville Island in the High Arctic (Fig. 1a). Herschel Island (Yukon, Canada) is located at 69°35' N and 139°05' W in the Beaufort Sea off the Yukon coast. The island is composed of unconsolidated and fine-grained marine and glaciogenic sediments as it was formed by the Laurentide Ice Sheet (Mackay, 1959; Pollard, 1990). The island is situated in the zone of continuous permafrost with ground ice content between 30 and 60 % for the entire island. Physical permafrost degradation typically occurs in the form of retrogressive thaw slumps (Lantuit and Pollard, 2008) and active layer detachments (Coch et al., in review). Ramage et al. (in review) reported mean active layer depths of 52.2 ± 20.2. Soil organic carbon content for valleys on the eastern side of Herschel Island was estimated to be 11.4 ± 3.7 kg m^2 at 0 - 30 cm depth and 26.4 ± 8.9 kg m^2 at 0 - 100 cm depth with a CN ratio of 12.9 ± 2.2 in 0 - 100 cm depth (Ramage et al., in review). The dominant vegetation type is lowland tundra (Myers-Smith et al., 2011; Smith et al., 1989) and can be classified into subzone E (CAVM, 2003), which corresponds to the Low Arctic. The mean annual air temperature and yearly precipitation between 1971 and 2000 at Komakuk Beach, the nearest long-term meteorological station ~40 km away from our study site, are -11 °C and 161.3 mm respectively. The mean July temperature is 7.8 °C and average precipitation is 27.3 mm (Environment and Climate Change Canada, 2018). Snowmelt is the largest hydrological event of the year occurring in May to early June. Summer baseflow from mid-June onwards is controlled by rainfall events (Coch et al., 2018). The active layer freezes up by mid-November (Burn, 2012). The studied catchments unofficially named Ice Creek West (1.4 km^2) and Ice Creek East (1.6 km^2) are adjacent to each other and merge into an alluvial fan before draining into the Beaufort Sea (Fig. 1b, Table 1). There are degrading ice-wedge polygons present in the headwaters of Ice Creek West (Coch et al., in review).

The Cape Bounty Arctic Watershed Observatory (CBAWO) is situated on the south coast of Melville Island (Nunavut, Canada) at 74° 55' N and 109° 35' W. The geology is characterized by Devonian sandstone and siltstone bedrock overlain by Quaternary marine and glacial sediments (Hodgson et al., 1984). The soils are categorized as cryosols with a thin organic horizon. The site is situated in the zone of continuous permafrost, and active layer depths typically range from 50 to 70 cm (Lafrenière et al., 2013). Permafrost degradation such as deep thaw and physical disturbances have altered hydrochemical fluxes of the rivers (Lamoureux and Lafrenière, 2017). The vegetation cover is patchy with polar semi-desert, mesic tundra and wet sedge

meadows (Edwards and Treitz, 2018), and falls into subzones B and C (CAVM, 2003). Soil organic carbon is estimated to be 3.0 kg m^2 in 0 - 30 cm depth, and 10.2 kg m^2 in 0 - 100 cm depth (Hugelius et al., 2013), with a CN ratio of 10.0 in 0 - 100 cm depth (ADAPT, 2014). The nearest long-term meteorological station is located ~ 300 km away, at Mould Bay (NWT). Between 1971 and 2000, the mean annual air temperature and precipitation were -17.5°C and 111 mm, respectively. Average July

5   temperature is 4.0 °C, whereas mean precipitation is 13.5 mm. Snowmelt and nival flow typically start in early to mid-June, whereas baseflow occurs around mid-July. Refreezing of the active layer starts mid- to late August (Lamoureux and Lafrenière, 2017; Lewis et al., 2012). Samples were taken downstream in Boundary River (152.5 km^2), its sub-catchment Robin Creek (14.8 km^2), and the neighboring watersheds West River (8.8 km^2) and East River (12.4 km^2) There is an active retrogressive thaw slump in the Robin Creek watershed, and a number of recent (since 2007) active layer detachments and other disturbances

10   in the West River watershed.

3 Methods

3.1 Field methods and hydrochemistry

Field work on Herschel was carried out in July-August 2016. We measured discharge using a cutthroat flume equipped with a U20 Onset Hobo level logger in Ice Creek West. Discharge data at 30 minute intervals is available from 15 May 2016 and at

15   5 minute intervals after 22 July 2016 (Coch et al., 2018; Coch et al., in review). In Ice Creek East, discharge was determined using the area velocity method in combination with a U20 Onset Hobo level logger (see Coch et al. in review for a detailed description). Data in Ice Creek East is available at 5 minute intervals after 25 July 2016. Weather data is available from the local Environment and Climate Change Canada Station, and from a station deployed in Ice Creek West during the summer. Water samples were collected at the outflow of both streams between 20 July and 10 August. At the outflow of Ice Creek

20   West, water samples were collected using an automatic water sampler (ISCO 3700) at a 12-hour interval between 25 July and 10 August and more frequently during rainfall events (between 1-3 hours). Prior to the automatic sampling, and also in Ice Creek East, water samples were taken manually. We collected water samples along longitudinal profiles of the channels starting in the headwaters (~ 2000 m distance from the outflow) and following the river downstream. This was done 3 times in Ice Creek West (20, 25 and 30 July) and once in Ice Creek East (30 July). Samples of flowing waters are available from Ice Creek

25   West (n=90), Ice Creek East (n=32) and the alluvial fan (n=8). Standing water samples (n=4) were collected from ponds in the Ice Creek West catchment.

The field work at Cape Bounty took place in August 2017. All water samples were collected manually after triple rinsing the sampling bottle. Similarly to the Herschel field work, we collected samples along longitudinal stream profiles. Robin Creek is a subcatchment of Boundary River (Fig. 1), where stream samples were collected at six locations downstream of a retrogressive

30   thaw slump. Three lakes were also sampled in the Boundary river catchment, and 2 samples from the main river channel. A total of 21 river samples and 9 samples from lakes and ponds are available from the West River catchment, some of which

were collected after the rainfall event on 12 August 2017. In East River, 4 samples are available from the stream and 8 samples from standing water bodies.

Within 24 hours of sampling, electrical conductivity and pH were measured in the field lab. After collection, water samples were filtered through pre-rinsed 0.7 µm GF/F syringe filters and where then stored cool and dark for transport to the Alfred-
5   Wegener-Institute, University of Hamburg and Geoscience Research Centre GFZ, Germany, where analysis for DOC and cDOM were carried out. Samples for DOC analyses were acidified with HCl (30 % suprapur) prior to the measurements. In 2016, DOC measurements were performed on a Shimadzu TOC-L analyzer with a TNM-L module (University of Hamburg), whereas a Shimadzu TOC-VCPH analyzer was used in 2017 (AWI). The error for these measurements is below 10 %. Inorganic carbon (TIC) was sparged out using synthetic air prior to the measurement. As we had a shortage of HCl in the field
10   in 2016, 82 of the samples were frozen and acidified upon return to Germany. After new acid was acquired later in the summer, sample duplicates (n=47) were processed directly in the field and also frozen. The frozen duplicate was thawed and acidified upon return to determine the effect of different sample treatment (Coch et al. 2018). There is a significant linear relationship ($p < 0.05$, n = 47, $R^2 = 0.87$) between DOC concentrations of unfrozen and frozen sample duplicates. Samples that were frozen in the field, and subsequently thawed and acidified upon return to Germany showed lower DOC concentrations (by 13%) than
15   samples that were acidified directly in the field and kept unfrozen. We corrected the frozen samples for this offset (Supplementary S1). In both years, deionized water used in the field was also analyzed as blank following the same procedure. The absorbance of cDOM was measured on a LAMBDA 950 UV/Vis Spectrophotometer (GFZ Potsdam) for the wavelength from 200 to 800 every 1 nm (average of duplicates) using a 5cm cuvette and Milli-Q water as a reference. Some of the water samples showed fine particles precipitated in the sample bottle. They appeared in the form of small thin flakes, which partly
20   remained in suspension or accumulated at the bottom of the flask. This precipitation occurred after the samples were filtered through 0.7 µm glass fiber filters and transported to the laboratory. This was noted down in the lab, and absorbance spectra were not further analyzed for those samples as interference of the spectral characteristics by the particles might have occurred. This was the case for 25 (out of 55) samples at Cape Bounty and for 8 samples (out of 134) at Herschel Island.

The Naperian spectral absorption coefficient of cDOM ($a_{cDOM}(\lambda)$) was calculated with
25   $$a_{CDOM}(\lambda)\ (m^{-1}) = \frac{2.303 * A_\lambda}{L}\ , \tag{1}$$

where A_λ is the absorbance and L the optical path length of the used cuvette in the spectrophotometer. The absorption was corrected for instrument drift and scatter using a baseline correction by subtracting $a_{cDOM}(700)$ (Hancke et al., 2014; Helms et al., 2008). At that wavelength, absorption by CDOM is assumed to be negligible (Mitchell et al, 2002). Spectral slopes of a_{cDOM} for wavelength ranges from 275 to 295nm (S275-295) and 350 to 400nm (S350-400) were calculated using Eq. (2) and
30   a non-linear fit. These slopes indicate photochemical or microbial alteration of DOM (Helms 2008). The ratio of both slopes (S275-295 : S350-400) defines the slope ratio (SR). The SUVA (mg L^{-1} m^{-1}) was calculated by dividing the decadal absorption (A_{254} / L) at 254 nm (m^{-1}) by DOC (mg l^{-1}). Both parameters have been related to the relative molecular weight and aromaticity of DOM (Helms et al., 2008; Weishaar et al., 2003).

$$a_{CDOM}(\lambda)(\lambda) = a_{CDOM}(\lambda_0) * e^{-S(\lambda - \lambda_0)}, \tag{2}$$

Where λ_0 is the absorption coefficient at reference wavelength and S is the spectral slope of $a_{CDOM}(\lambda)$ for the chosen wavelength range. To compare our data with different studies we converted absorption coefficient reported in various studies to $a_{cDOM}350$ using an interpolation method developed by Massicotte et al. (2017a).

3.2 Statistical Analyses

5 We used RStudio (Version 1.0.153) to perform statistical tests (RStudio Team, 2016). Normality was tested using the Shapiro-Wilk normality test. To determine the difference in means of two populations, we applied the Welch's two sample t-test if the data was normally distributed with unequal variances. In the case of not normally distributed data, we used the Wilcoxon-Mann-Whitney test. To measure the relationship between two variables, we used the Pearson correlation coefficient for normally distributed data and the Spearman rank correlation if the data was not normally distributed.

10 ## 4 Results

4.1 Meteorological conditions and general hydrochemistry

The mean annual air temperature on Herschel Island was -6.3 °C in 2016 with mean temperatures of 9.4 °C in July and 7.7 °C in August. During the monitoring period, rainfall events of 33.9 mm (19 July), 9.3 mm (30 July) and 12.7 mm (5 August) were recorded. CABWO had a mean annual air temperature of -15.3 °C in 2017, with mean air temperatures of 4.5 °C in July and

15 1.6 °C in August. During the monitoring period, two rainfall events of 0.2 mm (4 August) and 1.2 mm (8 August) occurred. Electrical conductivity (EC) and pH are significantly higher ($p < 0.05$) in surface waters on Herschel Island (1050 ± 370 µS cm^{-1} and 8.2 ± 0.2) than at Cape Bounty (137 ± 136 µS cm^{-1} and 7.2 ± 0.5). Whereas no difference was found for these parameters between standing and flowing water on Herschel Island, pH and EC were significantly higher in standing water at Cape Bounty than in flowing water (Table 2). Robin Creek showed highest EC values and the largest variability (145 ± 213

20 µS cm^{-1}) of the Cape Bounty rivers, whereas West River showed the overall lowest EC values (60 ± 17 µS cm^{-1}). On Herschel Island, both adjacent rivers show EC and pH values in the same order of magnitude with a slight decrease at the alluvial fan outflows.

4.2 DOC and CDOM absorption characteristics

CDOM absorption spectra between 250 and 700 nm follow different patterns on Herschel Island and Cape Bounty (Fig. 2).

25 Absorption is significantly higher ($p < 0.05$) on Herschel Island than on Cape Bounty across the entire spectrum. The absorption at 350 nm wavelength (Fig. 2b) is significantly higher on Herschel Island (14.5 ± 5.1 m^{-1}) than on Cape Bounty (5.5 ± 4.9 m^{-1}). The same applies to the CDOM slope S275-295, which amounts to 0.016 ± 0.001 on Herschel Island and 0.015 ± 0.003 on Cape Bounty.

We found a significant positive relationship (rho = 0.78, $p < 0.05$) between the cDOM absorption at 350 nm and DOC concentration for all samples at both sites (Fig. 3a). DOC in surface water samples from Herschel Island amounted to 10.0 ± 1.6 mg l^{-1} on average, which is significantly higher than DOC concentrations from Cape Bounty water samples (2.5 ± 2.0 mg l^{-1}). Comparing the rivers on Herschel Island (Fig. 3b), highest DOC and $a_{cDOM}350$ values were found in the headwaters of Ice

5   Creek West. Ice Creek West had significantly higher ($p < 0.05$) values in DOC 10.4 ± 1.5 mg l^{-1}) and $a_{cDOM}350$ (16.1 ± 5.4 m^{-1}) than Ice Creek East, which were 8.7 ± 1.1 mg l^{-1} and 11.1 ± 1.8 m^{-1}, respectively. No significant difference was found between the SUVA values for the two creeks. The relationship between $a_{cDOM}350$ and DOC at Cape Bounty is broadly separated into two groups, namely flowing and standing water. Both correlations are significant (< 0.05) and show different slopes (Fig. 3c). DOC and SUVA are significantly different for standing water relative to flowing water. No significant

10   difference between these water types was found for $a_{cDOM}350$. Within the group of standing water, samples from the East River catchment show the highest DOC and $a_{cDOM}350$ values. The highest values of DOC and $a_{cDOM}350$ values of flowing water were recorded in West River after the August 8 rainfall event.

There is a significant difference ($p < 0.05$) between the mean cDOM slopes S275-295 for samples from Herschel Island (0.016 ± 0.001 nm^{-1}) and Cape Bounty (0.015 ± 0.003 nm^{-1}). Compared to the SUVA values, we found a moderate significant

15   relationship between SUVA and the mean cDOM slopes all water samples from both locations (rho = -0.64, $p < 0.05$). The slopes on Herschel Island showed a narrow spread (Fig. 4b). This means that they remained within a small range with changing SUVA, except for two outliers in Ice Creek East. They exhibited a clear negative relationship (rho = -0.72, $p < 0.05$). The headwaters in both rivers showed slightly smaller slopes than the samples taken downstream. Samples from Cape Bounty (Fig. 4c) showed a negative relationship (rho = -0.66, $p < 0.05$) between SUVA and S275-295. Standing water samples showed

20   significantly larger slopes ($p < 0.05$) and significantly smaller SUVA ($p < 0.05$) than flowing water samples.

4.3. Downstream patterns of DOC and cDOM along longitudinal transects

The studied rivers on Herschel Island and Cape Bounty followed different hydrochemical patterns from upstream to downstream (Fig. 5). At Herschel Island, DOC concentration (Fig. 5a) decreased from upstream to downstream for Ice Creek West at all times of sampling, whereas it remained on a similar level from upstream to downstream in Ice Creek East. On 30

25   July 2016, when both rivers were sampled simultaneously, Ice Creek East showed significantly lower ($p < 0.05$) DOC concentrations than Ice Creek West throughout the entire profile. At Cape Bounty, DOC concentrations remain at a low level in all streams, except after the rainfall event in West River. Here, we found higher levels of DOC compared to the other rivers, and also a more pronounced downstream increase of DOC. East River shows a slight downstream decrease of DOC. In Robin Creek, we found an increase in DOC from 1.3 mg l^{-1} to 1.7 mg l^{-1} as the stream gets impacted by a retrogressive thaw slump.

30   DOC drops directly thereafter. No clear pattern was detected in Boundary river.

Similar patterns as for DOC were found for $a_{cDOM}350$. This confirms the relationship between both parameters (Fig. 3) which is especially high at Herschel Island. At Cape Bounty $a_{cDOM}350$ followed the same pattern as DOC in West River. For the remaining rivers, $a_{cDOM}350$ remained at a low level throughout the profiles.

SUVA values showed different trends in the rivers of Herschel Island and Cape Bounty (Fig. 5c). At Herschel Island, SUVA values remained at the same level along the profiles of both streams and did not show strong differences between rainfall and post rainfall conditions. In contrast, at Cape Bounty, West River (sampled after rainfall) showed higher SUVA than the remaining rivers (sampled before the rainfall). Further, an increase in SUVA downstream was visible in Robin Creek and Boundary River, although the number of available data points is limited.

Slope values at Herschel Island were variable in the headwaters and showed an increase downstream. They were smallest after the first rainfall event in Ice Creek West and increase progressively over the course of the season. We found lows in the headwaters of Ice Creek West at ~2000 and ~1250m distance from the outflow. Overall, Ice Creek West showed smaller slope values along the stream profile compared to Ice Creek East on 30 July 2016. The rivers on Cape Bounty showed highest slopes for East River (0.016 ± 0.001 nm^{-1}) and the lowest for West River ($0.012 \pm <0.001$). Robin Creek showed a decrease in slope from 0.017 nm^{-1} at ~2100 m distance to 0.014 nm^{-1} at the outflow. In contrast, a slight downstream increase in slope was recorded in West River.

Electrical conductivity was found to increase from upstream to downstream in Ice Creek West, whereas they remained at a similar level in ICE. It remained below 200 µS cm^{-1} at all times, except for the upstream location in Robin Creek where an active retrogressive thaw slump is hydrologically connected to the stream. It dropped substantially thereafter.

4.4 Temporal trends of DOC and cDOM with changing meteorological conditions

Changes over the summer season were observed for both rivers at Herschel Island (Fig. 6). Rainfall response is direct with steep rising hydrographs and elongated falling limbs in both streams (detailed presentation of rainfall response in Coch et al. 2018). After the peakflow following the 33.9 mm rainfall event (Event-1), both streams showed a decline in DOC accompanied by a decline in $a_{cDOM}350$, SUVA, and an increase in S275-295. EC is steadily increasing after peakflow in both streams.

The subsequent rainfall event (Event-2, 9.3 mm) led to an increase of DOC, $a_{cDOM}350$ and S275-295, and a drop in SUVA in Ice Creek West. This dynamic was not captured in Ice Creek East, which was sampled at a longer time interval. Baseflow had increased after this rainfall event (Fig. 6a).

The hydrochemical response to the following rainfall event (Event-3, 12.7 mm) was different to the previous one. Here, we saw an initial drop in DOC, $a_{cDOM}350$ and S275-295, and then an increase of these parameters in Ice Creek West. SUVA shows an increase with two positive peaks. Ice Creek East had a different response showing an increase in DOC and $a_{cDOM}350$ and a drop in SUVA. No continuous slope records are available for this event as two outliers occurred in this event.

5 Discussion

5.1 Limitations of cDOM measurements from terrestrial sources

There are a few constraints to optical DOM measurement that we encountered in this study. As described in the methods section, a number of samples showed precipitation inside the bottles in the form of small thin flakes, which partly remained in
5 suspension or accumulated at the bottom. All samples were filtered through 0.7 µm glass fiber filters, and the precipitation occurred after filtration. In the absorption spectra, these samples showed extraordinarily high a_{cDOM} values when compared to their DOC concentration level. As described in the methods section (3.1), they were therefore excluded from the study based on the laboratory notes. At Cape Bounty, this was the case for 25 out of 55 samples. Unfortunately, we do not have any supporting data for these sampling sites, such as dissolved solids or turbidity. We assume that high absorption values are a
10 result of multiple other absorbers beside cDOM and scattering by particles. This might have played a role also for other samples, even if they did not show precipitation in the sample bottles. We find that at Cape Bounty, 7 samples stand out in terms of higher $a_{cDOM}350$ compared to their DOC values – samples from West River and East River standing water (Fig. 3c). Possible influences of absorbance measurements are going to be discussed here.

The cut off between solid and dissolved fraction in a solution is normally made at 0.22, 45 µm or 0.7 µm depending on the
15 scientific community (e.g. among others, operational water quality, biogeochemistry, aquatic optics). Therefore, the operational definition of DOM varies between studies and the choice of the filter pore sizes. In our study, we filtered the water samples through 0.7 µm GF/F because this is the least organic-rich filter material and finest glass fibre filter that is offered on the market. Colloid complexes between 22 µm and 0.7 µm are in solution and may influence the absorbance spectra. Massicotte et al. (2017b) compared $a_{cDOM}(\lambda)$ for 1734 sample filtrates from different environments for its difference in 0.22 µm and 0.7
20 µm filter pore sizes. The result shows that water samples from environments with terrestrial dominated DOM are not as strongly affected as other water environments. Watanabe et al. (2015) found the difference between $a_{cDOM}(\lambda)$ between 0.22 µm and 0.7 µm to be about 12 %. Both studies conclude that the influence of different filter size on the absorbance spectra is relatively low. Most samples from our study were taken in streams of small watersheds with a clear terrestrial dominated DOM source. For most of our samples, we assume that the filter difference has a minor influence on cDOM absorption.

25 However, a possible source of absorption interference could be due to polymeric iron (hydr)oxides or high concentrations of dissolved iron. Iron (Fe(II,III)) is known to interfere with the absorption of cDOM (Poulin et al., 2014). Dissolved iron in terrestrially dominated waters is dominantly complexed with humic and fulvic acids. With changing temperature and changing pH of the sample filtrates, redox reaction can result in phase changes which then strongly affect the optical properties of the sample filtrate by scattering. We observed fine flakes in suspension or deposited at the bottom of some of the samples prior to
30 absorbance measurements. These particles could be precipitation of iron-organic acid colloids and thus a large source of overestimation of a_{cDOM} in those cases. Poulin et al. (2014) describes a linear dependency of increasing a_{cDOM} with increasing Fe(III) concentration in the water. The influence of iron is expected to be especially high in the spectral parameter of cDOM such as slopes and SR as well as SUVA. The study also showed that the fraction of Fe(II) and Fe(III) of the total iron

concentration inverts the two when pH increases from ~5.5 to 6.3. Table 2 shows the pH values for the different streams and catchments from this study. Lowest pH values were found in West River (6.9 ± 0.3), which is higher than the values reported by Poulin et al. (2014). This hypothesis needs thorough testing in a future study by analyzing dissolved solids along with optical characteristics. Poulin et al. (2014) further suggest to correct absorption coefficients according to the iron

5 concentrations using correction coefficients. For this study, only samples from Herschel Island were analyzed for total aqueous dissolved iron concentration. High total iron concentration is found to occur in high $a_{cDOM}350$ (Supplementary S2), which indicates an influence of iron concentration on the absorption. Fraction of Fe(II) and Fe(III) on the total iron concentration was not measured as a standard hydrochemistry measurement. Due to the lack of Fe hydrochemistry data from Cape Bounty, a uniform correction of all samples is therefore not possible. Therefore, all problematic samples were removed from this study.

10 **5.2 Catchment processes and biogeochemical cycling**

5.2.1 Regional catchment properties

Our both study sites show strong differences in DOM quantity and quality possibly related to their geographic location and environmental setting. Herschel Island (Low Arctic) shows on average significantly higher values in DOC, $a_{cDOM}350$, and SUVA, and lower values for S275-295 and SR than Cape Bounty (High Arctic). DOM in the Low Arctic is stronger coloured

15 (i.e. higher $a_{cDOM}350$) than in the High Arctic. This is a result of the greater abundance of plant material in the Low Arctic and a resulting high lignin concentration that can be introduced into the aquatic system (Sulzberger and Durisch-Kaiser, 2009).

The variability and range of SUVA and S275-195, indicating the molecular weight and aromaticity, is greater on Cape Bounty than it is on Herschel Island. The greater ranges of SUVA and S275-195 at Cape Bounty indicates a greater variability of DOM quality there. High SUVA in combination with low S275-195 indicate "fresh" DOM, or systems of shorter residence time

20 receiving a greater input of fresh DOM from the catchment area. In contrast, low SUVA and high S275-195 might be an indicator of limited fresh DOM inputs, a higher relative contribution of autochthonous DOM, greater exposure to photobleaching and longer residence time (Anderson and Stedmon, 2007; Fichot and Benner, 2012; Fichot et al., 2013; Helms et al., 2008; Whitehead et al., 2000).

In lakes, increased residence time of DOC in the system leads to a domination of partial photodegradation and an increase in

25 bacterial respiration. Only two standing water bodies (small ponds) at Herschel Island were sampled for DOC and optical properties. Although not statistically different, they showed higher $a_{cDOM}350$, DOC and S275-295 than flowing water bodies. At Cape Bounty, the difference between standing and flowing water bodies is more pronounced. Higher S275-295 and SR are explained by higher residence time resulting in more intense photodegradation and bacterial respiration. We will discuss downstream patterns in the different rivers in section 5.2.3.

5.2.2 Rainfall events

Rain plays an important role for mobilizing DOM from permafrost catchments. At Herschel Island, we captured three different rainfall events through continuous sampling at the outflow and repeated sampling along the longitudinal stream profile in Ice Creek West. Whereas the full response of rainfall event 1 was not captured at the outflow, the contrasting response of Ice

5   Creek West to rainfall events 2 and 3, suggests different sourcing of DOM. During the second rainfall event (9.3 mm), as DOC increased, we found a decrease in SUVA accompanied by an increase in S275-295. This indicates a decrease in aromaticity and a lower molecular weight, which suggests more decomposed, labile material. The following event of 12.7 mm led to a drop in DOC and S275-295 and a clear increase in SUVA indicating an increase in aromaticity and a higher molecular weight – suggesting more lignin rich plant derived DOM. A change in water sources for these two rainfall events was examined by

10   Coch et al. (in review). Whereas the 9.3 mm rainfall event showed the signature of supra-permafrost water, which was forced out during that rainfall event, the subsequent 12.7 mm rainfall event reflected the isotopic signature of rain. Thus, the DOM was first sourced through the entire active layer and had a longer residence time than the rain event after. This indicates that antecedent (pre-rainfall) conditions play a crucial role for the sourcing of DOM. The second rainfall event (9.3 mm) occurred about 10 days after the first one (33.9 mm), whereas the time difference between the second and the third one was less than 4

15   days. In addition to the antecedent conditions, the magnitude and intensity of the rainfall event might also play an important role here. The 9.3 mm rainfall event occurred over a period of 3 days. Thus, the flow pathways during this event might be deeper in the active layer mobilizing more decomposed OM (Marín-Spiotta et al., 2014). In contrast, the subsequent 12.7 mm event occurred within 1 day, which presumably led to increased overland flow and the mobilization of surface OM. Baseflow in this catchment is increasing with summer rainfall and as the summer season progresses (Coch et al., 2018). The authors also

20   reported a linear increase of DOC export with increasing runoff. Our dataset shows that the quality of exported DOC depends on the intensity of rainfall and the antecedent conditions, which in turn determine hydrological flow pathways and sourcing of DOM.

Although only one river was sampled before and after rainfall on Cape Bounty (West River), we found a tremendous increase in DOC there. Fouché et al. (2017) conducted an extensive study of DOM quality in four headwater streams of West River

25   (Cape Bounty) and also reported an increase in DOC concentrations and fluxes during stormflow. They observed a change in DOM quality: enrichment in fresh low molecular weight (LMW), microbially-derived, components as indicated by an increase in S275-295 and a decrease in SUVA during rainfall. Although we do not have data on the optical properties for West River before the rainfall event, similar concentrations of DOC in West River and East River point towards similar optical characteristics at that time. Baseflow in undisturbed High Arctic headwater streams seems therefore characterized by more

30   high molecular weight (HMW) humic-like components with high aromaticity (low slope and increase in SUVA) relative to stormflow DOM. In turn, stormflow leads to an export of DOM characterized by lower molecular weight and decreased aromaticity (high slope, decreased SUVA). Fouché et al. (2017) explain this pattern by a change in flow pathways from shallow active layer soils (baseflow) to subsurface runoff (rainfall), where soluble components from mineral soils deeper in the active

layer are mobilized. Associated with the change in DOM quality, they also found an increase in total dissolved solids (TDS) supporting this hypothesis. Impacts of changing flow pathways on DOM quality are also reported from a Subarctic setting by Balcarczyk et al. (2009). The increased residence time of percolating water through the active layer leads to a selective sorption of compounds to mineral soil particles. The authors describe that hydrophobic compounds are absorbed, while hydrophilic

5   compounds remain in the solution, and are therefore exported from the catchment (Balcarczyk et al., 2009). Further, an increased residence time and subsurface flow mobilizes DOC that is more microbially degraded (Striegl et al., 2005; Ward and Cory, 2015).

Different studies anticipate a shift towards deeper flow pathways as active layer depths increase with climate change (Mann et al., 2015; O'Donnell et al., 2014; Ward and Cory, 2015). These studies found that permafrost-derived DOM is more labile

10 compared to surface (organic mat) DOM. Here, we show that stormflow at the Low and High Arctic locations alter flow pathways and therefore the quality of DOM exported. At the Low Arctic setting our data suggests that more permafrost-derived DOM is exported with increasing baseflow during the season and during a rainfall event of smaller magnitude and lower intensity. In contrast, rainfall events of high magnitude and intensity that act on saturated soil lead to shorter residence time in the flow path and thus export more fresh near-surface-derived DOM (higher SUVA and lower S275-295). As summer rainfall

15 is projected to increase across the Arctic (Bintanja, 2018; Bintanja and Andry, 2017), we are expecting an increase in DOC export across the Arctic. The DOM quality will depend on the residence time and thus, flow pathways within the catchment, which in turn is controlled by the frequency and magnitude of the rainfall events and the thaw depth of the active layer.

5.2.3 Downstream patterns and impact of permafrost disturbance

Transport and degradation of DOC is a dynamic process. Vonk et al. (2015b) showed that the degradability decreased from

20 small streams towards larger rivers within the continuous permafrost zone. The fate of DOC along lateral flow pathways from headwater streams through lakes and large rivers to the ocean is connected to photochemical and biological oxidation (Cory et al., 2015; Cory et al., 2014). Studies show the importance of headwater systems where photodegradation (Cory et al., 2014) and bacterial respiration of ancient permafrost-derived DOC are prevalent (Mann et al., 2015). Our objective was therefore to investigate the upstream to downstream patterns in small coastal catchments in the Low and High Arctic.

25 At Herschel Island, we found a high variability of DOC, SUVA and S275-295 in the headwaters of Ice Creek West. The locations at 2000 m and 1300 m distance from the outflow show high DOC, S275-295 and low SUVA compared to the other locations. There are degrading ice-wedge polygons present, which heavily influence the headwaters of the stream. The location at 1300 m marks the inflow of another headwater tributary where degrading ice-wedge polygons are present. Thus, main expected sources for fresh mobilized DOM are headwaters and water from the tributary. This is clearly reflected in DOC and

30 $a_{cDOM}350$ with highest values in the headwaters and decreasing towards the outflow with another peak at the location of the tributary inflow. S275-295 shows a gradually photochemical degradation of DOM with distance and an interruption where fresh DOM is provided by the tributary channel (1300m). S275-295 has been found a good indicator for photodegradation of DOM (Fichot and Benner, 2012; Fichot et al., 2013; Helms et al., 2008), and also been observed along a flow-path continuum

of the Kolyma river basin (Frey et al., 2016). Here, they found a relative constant proportion of bioavailable DOC along the entire flow path, indicating an acclimatization of aquatic microorganisms to downstream DOM changes and/or the generation of labile DOM for microbial processing through photodegradation. SUVA values show a similar pattern to DOC and $a_{cDOM}350$ including the distinct increase at 1300m. In Ice Creek East, the influence of degrading ice-wedge polygons is minimal, so that

5   we do not see a clear downstream pattern of DOC. At locations where ice-wedge polygon degradation is present, we see a high aromaticity and higher molecular weight than further downstream from that location. We assume that microbial and photochemical degradation or both processes are altering the DOM downstream. Cory et al. (2014, 2015) show at a Subarctic site that DOC in headwater streams, which are directly sourced by soil water, have low prior exposure to light and is therefore prone to photodegradation to CO_2.

10 At Cape Bounty, optical data of upstream to downstream patterns is more limited (see section 5.3). West River shows an increase in DOC downstream after the rainfall event (3 August 2017), which is also reflected in an increase of $a_{cDOM}350$. As discussed by Fouché et al. (2017) and Wang et al. (2018), West river is characterized by a downstream increase in autochthonous DOM. SUVA and S275-295 do not show strong differences downstream in the West River. The adjacent catchment East River shows a smaller cDOM slope at the location 4000 m from the outflow, accompanied with an increase in

15 SUVA and low DOC concentration. The greatest measured differences are found in Robin Creek, which represents the outflow from an active retrogressive thaw slump. At ~2100 m distance from the outflow, closest to the slump, we see the highest DOC, S275-295 and EC values and lowest SUVA. This is indicative of low aromaticity and lower molecular weight. Downstream of this point, at the outflow of Robin Creek draining into Boundary river, high SUVA and a shallow S275-295 are found. The first sampling point, at about 1600 m upstream marks the point before both rivers merge. It is visible, that, after Robin Creek

20 merges SUVA increased downstream. This reflects low aromaticity downstream. Abbott et al. (2014) found that DOM is most biodegradable during active disturbance at sites in the Subarctic. SUVA values at thermokarst outflows in that study are half as high as in undisturbed reference waters indicating less aromatic DOC. Fouché et al. (2017), who studied headwater streams of West River found greater microbial activity with an increase in the magnitude of geomorphic disturbance indicated by an increase of less-humified and degradable protein-like components. S275-295 and SR significantly increased in those cases.

25 Impact of retrogressive thaw slumps on DOM quality was also studied in the Subarctic Peel Plateau by Littlefair et al. (2017). They reported similar dynamics at modestly sized slumps as we observed at Robin Creek: DOC concentration is highest directly at the slump outflow and is lower downstream compared to the undisturbed site before the slump impacted the stream. The authors attribute low SUVA and high S275-295 within the disturbed site to deep permafrost flow pathways. Our SUVA values within the slump and downstream are very similar to the ones reported by Littlefair et al. (2017), despite the great

30 geographical difference.

5.3 Nature of cDOM-DOC across the terrestrial Arctic

There is a strong relationship between DOC and $a_{cDOM}350$ across our study sites, which has been reported previously for the large Arctic rivers by Walker et al. (2013), and globally by Massicotte et al. (2017a). Breton et al. (2009) report DOC and

cDOM values for thaw ponds in northeastern Canada across different vegetation zones, and this data is also available from Scandinavia (Forsström et al., 2015; Kellerman et al., 2015) and the Alaskan Arctic (Cory et al., 2015; Larouche et al., 2015). Comparing our sites to those found in the literature confirms the strong positive relationship (rho = 0.85, p < 0.05) between DOC and $a_{cDOM}350$ (Fig. 7). This means that the optical parameter a_{cDOM} acts as a good proxy for DOC concentration. The

5 highest values for DOC and $a_{cDOM}350$ are found in Sweden (Kellerman et al., 2015) and the Canadian Subarctic (Breton et al., 2009). Figure 8 includes also sites from Siberia (Dvornikov et al., 2018; Skorospekhova et al., 2016; Skorospekhova et al., 2017), where only $a_{cDOM}350$ is available. There is a weak significant negative relationship between latitude and $a_{cDOM}350$ (rho = -0.22, p < 0.05) pointing towards a decrease in cDOM and therefore DOC as going north. The great variability of $a_{cDOM}350$ within study regions is especially visible in Yamal and Scandinavia, where a large range of absorption values is covered

10 independent from latitude. This is due to different catchment sizes of the water bodies sampled.

It is remarkable that the DOC-$a_{cDOM}350$ relationships from surface water bodies across the Arctic are similar to the one established for the five large Arctic rivers (Mackenzie, Lena, Kolyma, Ob', Yenisei) (Fig. 7, Walker et al. (2013)). The authors also report SUVA for three different flow regimes: peakflow (spring freshet), midflow (summer) and baseflow (winter). The SUVA values reported in this study (2.9 ± 0.4 L mg^{-1} m^{-1} for Herschel Island and 2.8 ± 1.1 L mg^{-1} m^{-1} for Cape Bounty) are

15 higher than the mean mid-flow SUVA for the five Arctic rivers (2.4 L mg^{-1} m^{-1}), which ranges between 2.0 L mg^{-1} m^{-1} in the Mackenzie River and 2.7 L mg^{-1} m^{-1} in the Ob'. This confirms the hypothesis proposed by Vonk et al. (2015b), that DOM exported from smaller rivers has a higher aromaticity, which suggests that the material is fresh and prone to degradation.

We linked cDOM and $a_{cDOM}350$ from this study and the literature (Table 3; Supplementary Table S1, S2) to latitude and the soil organic carbon content (SOCC) in 0-30 cm and 0-100 cm depth as retrieved from Hugelius et al. (2013). We found a

20 positive correlation (rho = 0.53/0.51, p < 0.05) between SOCC and DOC concentration. The relationship between $a_{cDOM}350$ and SOCC is also significant, although weaker (rho = 0.26 / 0.34, p < 0.05). It is important to bear in mind that the northern circumpolar soil carbon database is a product of upscaling and will most likely not cover the spatial variability reported in the studies.

6 Conclusion

25 This study investigates DOM optical properties in Low and High Arctic surface water environments and downstream patterns with regard to permafrost disturbance and rainfall events. We find that both Arctic locations exhibit a distinct signature of DOC concentration and $a_{cDOM}350$ linked to the differences in vegetation cover and SOCC content. Compared to the High Arctic, DOM in the Low Arctic is stronger coloured due to the greater abundance of plant material and higher lignin concentrations introduced into the aquatic system. SOCC is higher in the Low Arctic than in the High Arctic. This results in

30 higher DOC and $a_{cDOM}350$ values in the Low Arctic (Herschel Island) than in the High Arctic (Cape Bounty).

In both regions, the strong terrestrial signature of DOM is apparent in the optical properties, which is typical for small headwater catchments. The relationship between $a_{cDOM}350$ and DOC is very strong across both regions and including data

from the literature, proving the applicability of cDOM as a tracer for DOC throughout different aquatic Arctic environments (rivers, streams and lakes). It agrees very well with the $a_{cDOM}350$ to DOC relationship established for the great five Arctic rivers. However, examining DOM optical characteristics (SUVA, S275-295 and SR) for those large rivers and our sites, we find that smaller catchments in our study deliver fresher DOM prone to degradation.

5 The optical characteristics of DOM prove also a useful tool for assessing downstream patterns in the streams studied. The downstream increase of S275-295 is indicative for photodegradation processes, which is apparent in most of the streams. Further, local sources of DOM such as degrading ice-wedge polygons are detected in the optical signature of DOM. Although the temporal resolution of data at Cape Bounty is limited, we found a similar response to rainfall events. Rainfall leading to runoff with a short residence time (rainfall of high magnitude and intensity, dry antecedent conditions in the catchment) leads

10 to the export of fresh near-surface-derived DOM (higher SUVA, lower S275-295). In contrast, baseflow conditions and long residence times (including low magnitude rainfall events and a saturated catchment) favors the export of permafrost-derived DOM that has undergone microbial processing in the soil. Examining flow pathways and residence time will be crucial to assess the impacts of projected increasing summer rainfall across the Arctic. Optical properties of DOM will be a useful tool for assessing DOM sources and quality.

15

Data Availability

Data has been made available through PANGAEA:

Coch, Caroline; Juhls, Bennet; Lamoureux, Scott; Lafrenière, Melissa; Fritz, Michael; Heim, Birgit; Lantuit, Hugues (2019): Colored dissolved organic matter (cDOM) absorption measurements in terrestrial waters on Herschel Island (Low Arctic) and

20 Melville Island (High Arctic) in 2016 and 2017. PANGAEA, https://doi.pangaea.de/10.1594/PANGAEA.897289

Author Contributions

C.C., H.L. and S.L. developed the study design. Field work was conducted by C.C. in 2016, and by C.C., S.L., M.L. in 2017. M.F. partly funded and supervised lab analyzes for cDOM measurements. B.J. processed the absorbance spectra and contributed to developing the manuscript. C.C. ran lab analyzes, processed and visualized the data with input from B.H., M.L.,

25 S.L. and H.L. and prepared the manuscript with editorial contributions from all co-authors.

Competing interests

The authors declare that they have no conflict of interest.

Biogeosciences
Discussions

Open Access

EGU

Acknowledgements

References

Abbott, B. W., Larouche, J. R., Jones, J. B., Bowden, W. B., and Balser, A. W.: Elevated dissolved organic carbon biodegradability from thawing and collapsing permafrost, J Geophys Res Biogeosci, 119, 2049-2063, 10.1002/2014jg002678, 2014.

ADAPT: Carbon, nitrogen and water content of the active layer from sites across the Canadian Arctic Nordicana D21, 10.5885/45327AD-

20 5245D08606AB4F52, 2014.

Aiken, G. R.: Fluorescence and dissolved organic matter: A chemist's perspective: Chapter 2, 35-74, 10.1017/CBO9781139045452.005, 2014.

Anderson, N. J., and Stedmon, C. A.: The effect of evapoconcentration on dissolved organic carbon concentration and quality in lakes of SW Greenland, Freshw. Biol., 52, 280-289, 10.1111/j.1365-2427.2006.01688.x, 2007.

25 Balcarczyk, K. L., Jones, J. B., Jaffé, R., and Maie, N.: Stream dissolved organic matter bioavailability and composition in watersheds underlain with discontinuous permafrost, Biogeochemistry, 94, 255-270, 10.1007/s10533-009-9324-x, 2009.

Bintanja, R., and Andry, O.: Towards a rain-dominated Arctic, Nat Clim Chang, 7, 263-267, 10.1038/nclimate3240, 2017.

Bintanja, R.: The impact of Arctic warming on increased rainfall, Sci. Rep., 8, 16001, 10.1038/s41598-018-34450-3, 2018.

Breton, J., Prairie, Y., Vallières, C., and Laurion, I.: Limnological properties of permafrost thaw ponds in northeastern Canada, Can. J. Fish.

30 Aquat. Sci., 66, 1635-1648, 10.1139/f09-108, 2009.

Burn, C. R.: Herschel Island Qikiqtaryuk: A Natural and Cultural History of Yukon's Arctic Island, edited by: Burn, C. R., University of Calgary Press, 242 pp., 2012.

CAVM: Circumpolar Arctic Vegetation Map, Fish and Wildlife Service, Anchorage, Alaska, 2003.

Coch, C., Lamoureux, S. F., Knoblauch, C., Eischeid, I., Fritz, M., Obu, J., and Lantuit, H.: Summer rainfall DOC, solute and sediment

35 fluxes in a small Arctic coastal catchment on Herschel Island (Yukon Territory, Canada), Arctic Science, 10.1139/as-2018-0010, 2018.

Coch, C., Ramage, J. L., Lamoureux, S., Knoblauch, C., Meyer, H., and Lantuit, H.: Spatial variability of dissolved organic carbon (DOC), solutes and suspended sediment in disturbed Low Arctic coastal watersheds. , J Geophys Res Biogeosci, in review.

Cory, R. M., Ward, C. P., Crump, B. C., and Kling, G. W.: Carbon cycle. Sunlight controls water column processing of carbon in arctic fresh

40 waters, Science, 345, 925-928, 10.1126/science.1253119, 2014.

Cory, R. M., Harrold, K. H., Neilson, B. T., and Kling, G. W.: Controls on dissolved organic matter (DOM) degradation in a headwater stream: the influence of photochemical and hydrological conditions in determining light-limitation or substrate-limitation of photo-degradation, Biogeosciences, 12, 6669-6685, 10.5194/bg-12-6669-2015, 2015.

Dvornikov, Y., Leibman, M., Heim, B., Bartsch, A., Herzschuh, U., Skorospekhova, T., Fedorova, I., Khomutov, A., Widhalm, B., Gubarkov, A., and Rößler, S.: Terrestrial CDOM in Lakes of Yamal Peninsula: Connection to Lake and Lake Catchment Properties, Remote Sensing, 10, 10.3390/rs10020167, 2018.

Edwards, R., and Treitz, P.: Vegetation Greening Trends at Two Sites in the Canadian Arctic: 1984–2015, Arct. Antarct. Alp. Res., 49, 601-619, 10.1657/aaar0016-075, 2018.

Environment and Climate Change Canada, Historical Data: http://climate.weather.gc.ca/historical_data/search_historic_data_e.html, access: 12 December 2018, 2018.

Fichot, C. G., and Benner, R.: The spectral slope coefficient of chromophoric dissolved organic matter (S 275-295) as a tracer of terrigenous dissolved organic carbon in river-influenced ocean margins, Limnol. Oceanogr., 57, 1453-1466, 10.4319/lo.2012.57.5.1453, 2012.

Fichot, C. G., Kaiser, K., Hooker, S. B., Amon, R. M., Babin, M., Belanger, S., Walker, S. A., and Benner, R.: Pan-Arctic distributions of continental runoff in the Arctic Ocean, Sci. Rep., 3, 1053, 10.1038/srep01053, 2013.

Forsström, L., Rautio, M., Cusson, M., Sorvari, S., Albert, R.-L., Kumagai, M., and Korhola, A.: Dissolved organic matter concentration, optical parameters and attenuation of solar radiation in high-latitude lakes across three vegetation zones, Ecoscience, 22, 17-31, 10.1080/11956860.2015.1047137, 2015.

Fouché, J., Lafrenière, M. J., Rutherford, K., and Lamoureux, S.: Seasonal hydrology and permafrost disturbance impacts on dissolved organic matter composition in High Arctic headwater catchments, Arctic Science, 3, 378-405, 10.1139/as-2016-0031, 2017.

Frey, K. E., and Smith, L. C.: Amplified carbon release from vast West Siberian peatlands by 2100, Geophys. Res. Lett., 32, Artn L09401 10.1029/2004gl022025, 2005.

Frey, K. E., Sobczak, W. V., Mann, P. J., and Holmes, R. M.: Optical properties and bioavailability of dissolved organic matter along a flow-path continuum from soil pore waters to the Kolyma River mainstem, East Siberia, Biogeosciences, 13, 2279-2290, 10.5194/bg-13-2279-2016, 2016.

Green, S. A., and Blough, N. V.: Optical absorption and fluorescence properties of chromophoric dissolved organic matter in natural waters, Limnol. Oceanogr., 39, 1903-1916, 10.4319/lo.1994.39.8.1903, 1994.

Helms, J. R., Stubbins, A., Ritchie, J. D., Minor, E. C., Kieber, D. J., and Mopper, K.: Absorption spectral slopes and slope ratios as indicators of molecular weight, source, and photobleaching of chromophoric dissolved organic matter, 2008.

Hodgson, D. A., Vincent, J. S., and Fyles, J. G.: Quaternary geology of central Melville Island, Northwest Territories. Geological Survey of Canada, 10.4095/119784, 1984.

Holmes, R. M., McClelland, J. W., Peterson, B. J., Tank, S. E., Bulygina, E., Eglinton, T. I., Gordeev, V. V., Gurtovaya, T. Y., Raymond, P. A., Repeta, D. J., Staples, R., Striegl, R. G., Zhulidov, A. V., and Zimov, S. A.: Seasonal and Annual Fluxes of Nutrients and Organic Matter from Large Rivers to the Arctic Ocean and Surrounding Seas, Estuar. Coasts, 35, 369-382, 10.1007/s12237-011-9386-6, 2012.

Hugelius, G., Tarnocai, C., Broll, G., Canadell, J. G., Kuhry, P., and Swanson, D. K.: The Northern Circumpolar Soil Carbon Database: spatially distributed datasets of soil coverage and soil carbon storage in the northern permafrost regions, Earth System Science Data, 5, 3-13, 10.5194/essd-5-3-2013, 2013.

Hugelius, G., Strauss, J., Zubrzycki, S., Harden, J. W., Schuur, E. A. G., Ping, C. L., Schirrmeister, L., Grosse, G., Michaelson, G. J., Koven, C. D., amp, apos, Donnell, J. A., Elberling, B., Mishra, U., Camill, P., Yu, Z., Palmtag, J., and Kuhry, P.: Estimated stocks of circumpolar permafrost carbon with quantified uncertainty ranges and identified data gaps, Biogeosciences, 11, 6573-6593, 10.5194/bg-11-6573-2014, 2014.

Kellerman, A. M., Kothawala, D. N., Dittmar, T., and Tranvik, L. J.: Persistence of dissolved organic matter in lakes related to its molecular characteristics, Nat. Geosci., 8, 454-457, 10.1038/ngeo2440, 2015.

Lacelle, D., Bjornson, J., and Lauriol, B.: Climatic and geomorphic factors affecting contemporary (1950-2004) activity of retrogressive thaw slumps on the Aklavik Plateau, Richardson Mountains, NWT, Canada, Permafr. Periglac. Proc., 21, 1-15, 10.1002/ppp.666, 2010.

Lafrenière, M. J., and Lamoureux, S. F.: Thermal Perturbation and Rainfall Runoff have Greater Impact on Seasonal Solute Loads than Physical Disturbance of the Active Layer, Permafr. Periglac. Proc., 24, 241-251, 10.1002/ppp.1784, 2013.

Lafrenière, M. J., Laurin, E., and Lamoureux, S. F.: The Impact of Snow Accumulation on the Active Layer Thermal Regime in High Arctic Soils, Vadose Zone J., 12, 10.2136/vzj2012.0058, 2013.

Lamoureux, S. F., and Lafrenière, M. J.: Fluvial Impact of Extensive Active Layer Detachments, Cape Bounty, Melville Island, Canada, Arct. Antarct. Alp. Res., 41, 59-68, 10.1657/1938-4246(08-030)[lamoureux]2.0.co;2, 2009.

Lamoureux, S. F., and Lafrenière, M. J.: More than just snowmelt: integrated watershed science for changing climate and permafrost at the Cape Bounty Arctic Watershed Observatory, WIREs Water, 5, e1255, 10.1002/wat2.1255, 2017.

Lantuit, H., and Pollard, W. H.: Fifty years of coastal erosion and retrogressive thaw slump activity on Herschel Island, southern Beaufort Sea, Yukon Territory, Canada, Geomorphology, 95, 84-102, 10.1016/j.geomorph.2006.07.040, 2008.

Larouche, J. R., Abbott, B. W., Bowden, W. B., and Jones, J. B.: The role of watershed characteristics, permafrost thaw, and wildfire on dissolved organic carbon biodegradability and water chemistry in Arctic headwater streams, Biogeosciences, 12, 4221-4233, 10.5194/bg-12-4221-2015, 2015.

Le Fouest, V., Matsuoka, A., Manizza, M., Shernetsky, M., Tremblay, B., and Babin, M.: Towards an assessment of riverine dissolved organic carbon in surface waters of the western Arctic Ocean based on remote sensing and biogeochemical modeling, Biogeosciences, 15, 1335-1346, 10.5194/bg-15-1335-2018, 2018.

Lewis, T., Lafrenière, M. J., and Lamoureux, S. F.: Hydrochemical and sedimentary responses of paired High Arctic watersheds to unusual climate and permafrost disturbance, Cape Bounty, Melville Island, Canada, Hydrol. Processes, 26, 2003-2018, 10.1002/hyp.8335, 2012.

Lewkowicz, A. G.: Dynamics of active-layer detachment failures, Fosheim Peninsula, Ellesmere Island, Nunavut, Canada, Permafr. Periglac. Proc., 18, 89-103, 10.1002/ppp.578, 2007.

Littlefair, C. A., Tank, S. E., and Kokelj, S. V.: Retrogressive thaw slumps temper dissolved organic carbon delivery to streams of the Peel Plateau, NWT, Canada, Biogeosciences, 14, 5487-5505, 10.5194/bg-14-5487-2017, 2017.

Mackay, J. R.: Glacier ice-thrust features of the Yukon coast, Geographical Bulletin, 13, 5-21, 1959.

Mann, P. J., Davydova, A., Zimov, N., Spencer, R. G. M., Davydov, S., Bulygina, E., Zimov, S., and Holmes, R. M.: Controls on the composition and lability of dissolved organic matter in Siberia's Kolyma River basin, J Geophys Res Biogeosci, 117, 10.1029/2011jg001798, 2012.

Mann, P. J., Eglinton, T. I., McIntyre, C. P., Zimov, N., Davydova, A., Vonk, J. E., Holmes, R. M., and Spencer, R. G.: Utilization of ancient permafrost carbon in headwaters of Arctic fluvial networks, Nat Commun, 6, 7856, 10.1038/ncomms8856, 2015.

Marín-Spiotta, E., Gruley, K. E., Crawford, J., Atkinson, E. E., Miesel, J. R., Greene, S., Cardona-Correa, C., and Spencer, R. G. M.: Paradigm shifts in soil organic matter research affect interpretations of aquatic carbon cycling: transcending disciplinary and ecosystem boundaries, Biogeochemistry, 117, 279-297, 10.1007/s10533-013-9949-7, 2014.

Massicotte, P., Asmala, E., Stedmon, C., and Markager, S.: Global distribution of dissolved organic matter along the aquatic continuum: Across rivers, lakes and oceans, Sci. Total Environ., 609, 180-191, 10.1016/j.scitotenv.2017.07.076, 2017a.

Massicotte, P., Stedmon, C., and Markager, S.: Spectral signature of suspended fine particulate material on light absorption properties of CDOM, Mar. Chem., 196, 98-106, 10.1016/j.marchem.2017.07.005, 2017b.

Myers-Smith, I. H., Hik, D. S., Kennedy, C., Cooley, D., Johnstone, J. F., Kenney, A. J., and Krebs, C. J.: Expansion of Canopy-Forming Willows Over the Twentieth Century on Herschel Island, Yukon Territory, Canada, Ambio, 40, 610-623, 10.1007/s13280-011-0168-y, 2011.

Neff, J. C., Finlay, J. C., Zimov, S. A., Davydov, S. P., Carrasco, J. J., Schuur, E. A. G., and Davydova, A. I.: Seasonal changes in the age and structure of dissolved organic carbon in Siberian rivers and streams, Geophys. Res. Lett., 33, 10.1029/2006gl028222, 2006.

O'Donnell, J. A., Aiken, G. R., Walvoord, M. A., Raymond, P. A., Butler, K. D., Dornblaser, M. M., and Heckman, K.: Using dissolved organic matter age and composition to detect permafrost thaw in boreal watersheds of interior Alaska, J Geophys Res Biogeosci, 119, 2155-2170, 10.1002/2014jg002695, 2014.

Osterkamp, T. E.: Characteristics of the recent warming of permafrost in Alaska, J. Geophys. Res., 112, 10.1029/2006jf000578, 2007.

Pollard, W. H.: The nature and origin of ground ice in the Herschel Island area, Yukon Territory, Proceedings, Fifth Canadian Permafrost Conference, Québec, 23-30, 1990.

Poulin, B. A., Ryan, J. N., and Aiken, G. R.: Effects of iron on optical properties of dissolved organic matter, Environ. Sci. Technol., 48, 10098-10106, 10.1021/es502670r, 2014.

Ramage, J. L., Irrgang, A. M., Morgenstern, A., and Lantuit, H.: Increasing coastal slump activity impacts the release of sediment and organic carbon into the Arctic Ocean, Biogeosciences, 15, 1483-1495, 10.5194/bg-15-1483-2018, 2018.

Ramage, J. L., Fortier, D., Hugelius, G., Lantuit, H., and Morgenstern, A.: Distribution of carbon and nitrogen along hillslopes in three valleys on Herschel Island, Yukon Territory, Canada Catena, in review.

Schaefer, K., Lantuit, H., Romanovsky, V. E., Schuur, E. A. G., and Witt, R.: The impact of the permafrost carbon feedback on global climate, Environ Res Lett, 9, 085003, 10.1088/1748-9326/9/8/085003, 2014.

Smith, C. A. S., Kennedy, C. E., Hargrave, A. E., and McKenna, K. M.: Soil and vegetation of Herschel Island, Yukon Territory, Ottawa, ON, 101, 1989.

Spence, C., Kokelj, S. V., Kokelj, S. A., McCluskie, M., and Hedstrom, N.: Evidence of a change in water chemistry in Canada's subarctic associated with enhanced winter streamflow, J Geophys Res Biogeosci, 120, 113-127, 10.1002/2014jg002809, 2015.

Spencer, R. G. M., Aiken, G. R., Wickland, K. P., Striegl, R. G., and Hernes, P. J.: Seasonal and spatial variability in dissolved organic matter quantity and composition from the Yukon River basin, Alaska, Global Biogeochem. Cycles, 22, n/a-n/a, 10.1029/2008gb003231, 2008.

Spencer, R. G. M., Aiken, G. R., Butler, K. D., Dornblaser, M. M., Striegl, R. G., and Hernes, P. J.: Utilizing chromophoric dissolved organic matter measurements to derive export and reactivity of dissolved organic carbon exported to the Arctic Ocean: A case study of the Yukon River, Alaska, Geophys. Res. Lett., 36, 10.1029/2008gl036831, 2009.

Stedmon, C. A., Amon, R. M. W., Rinehart, A. J., and Walker, S. A.: The supply and characteristics of colored dissolved organic matter (CDOM) in the Arctic Ocean: Pan Arctic trends and differences, Mar. Chem., 124, 108-118, 10.1016/j.marchem.2010.12.007, 2011.

Striegl, R. G., Aiken, G. R., Dornblaser, M. M., Raymond, P. A., and Wickland, K. P.: A decrease in discharge-normalized DOC export by the Yukon River during summer through autumn, Geophys. Res. Lett., 32, 10.1029/2005gl024413, 2005.

5 Sulzberger, B., and Durisch-Kaiser, E.: Chemical characterization of dissolved organic matter (DOM): A prerequisite for understanding UV-induced changes of DOM absorption properties and bioavailability, Aquat. Sci., 71, 104-126, 10.1007/s00027-008-8082-5, 2009.

Tank, S. E., Fellman, J. B., Hood, E., and Kritzberg, E. S.: Beyond respiration: Controls on lateral carbon fluxes across the terrestrial-aquatic interface, Limnol Oceanogr Lett, 10.1002/lol2.10065, 2018.

Vonk, J. E., Tank, S. E., Bowden, W. B., Laurion, I., Vincent, W. F., Alekseychik, P., Amyot, M., Billet, M. F., Canário, J., Cory, R. M.,
10   Deshpande, B. N., Helbig, M., Jammet, M., Karlsson, J., Larouche, J., MacMillan, G., Rautio, M., Walter Anthony, K. M., and Wickland, K. P.: Reviews and syntheses: Effects of permafrost thaw on Arctic aquatic ecosystems, Biogeosciences, 12, 7129-7167, 10.5194/bg-12-7129-2015, 2015a.

Vonk, J. E., Tank, S. E., Mann, P. J., Spencer, R. G. M., Treat, C. C., Striegl, R. G., Abbott, B. W., and Wickland, K. P.: Biodegradability of dissolved organic carbon in permafrost soils and aquatic systems: a meta-analysis, Biogeosciences, 12, 6915-6930, 10.5194/bg-
15   12-6915-2015, 2015b.

Walker, S. A., Amon, R. M. W., and Stedmon, C. A.: Variations in high-latitude riverine fluorescent dissolved organic matter: A comparison of large Arctic rivers, J Geophys Res Biogeosci, 118, 1689-1702, 10.1002/2013JG002320, 2013.

Wang, Y., Spencer, R. G. M., Podgorski, D. C., Kellerman, A. M., Rashid, H., Zito, P., Xiao, W., Wei, D., Yang, Y., and Xu, Y.: Spatiotemporal transformation of dissolved organic matter along an alpine stream flow path on the Qinghai–Tibet Plateau:
20   importance of source and permafrost degradation, Biogeosciences, 15, 6637-6648, 10.5194/bg-15-6637-2018, 2018.

Ward, C. P., and Cory, R. M.: Chemical composition of dissolved organic matter draining permafrost soils, Geochim. Cosmochim. Acta, 167, 63-79, 10.1016/j.gca.2015.07.001, 2015.

Ward, C. P., Nalven, S. G., Crump, B. C., Kling, G. W., and Cory, R. M.: Photochemical alteration of organic carbon draining permafrost soils shifts microbial metabolic pathways and stimulates respiration, Nat Commun, 8, 772, 10.1038/s41467-017-00759-2, 2017.

25 Watanabe, S., Laurion, I., Markager, S., and Vincent, W. F.: Abiotic control of underwater light in a drinking water reservoir: Photon budget analysis and implications for water quality monitoring, Water Resour. Res., 51, 6290-6310, 10.1002/2014wr015617, 2015.

Weishaar, J. L., Aiken, G. R., Bergamaschi, B. A., Fram, M. S., Fujii, R., and Mopper, K.: Evaluation of Specific Ultraviolet Absorbance as an Indicator of the Chemical Composition and Reactivity of Dissolved Organic Carbon, Environ. Sci. Technol., 37, 4702-4708, 10.1021/es030360x, 2003.

30 Whitehead, R. F., de Mora, S., Demers, S., Gosselin, M., Monfort, P., and Mostajir, B.: Interactions of ultraviolet-B radiation, mixing, and biological activity on photobleaching of natural chromophoric dissolved organic matter: A mesocosm study, Limnol. Oceanogr., 45, 278-291, 10.4319/lo.2000.45.2.0278, 2000.

Woo, M.-K., Kane, D. L., Carey, S. K., and Yang, D.: Progress in permafrost hydrology in the new millennium, Permafr. Periglac. Proc., 19, 237-254, 10.1002/ppp.613, 2008.

35

Figures
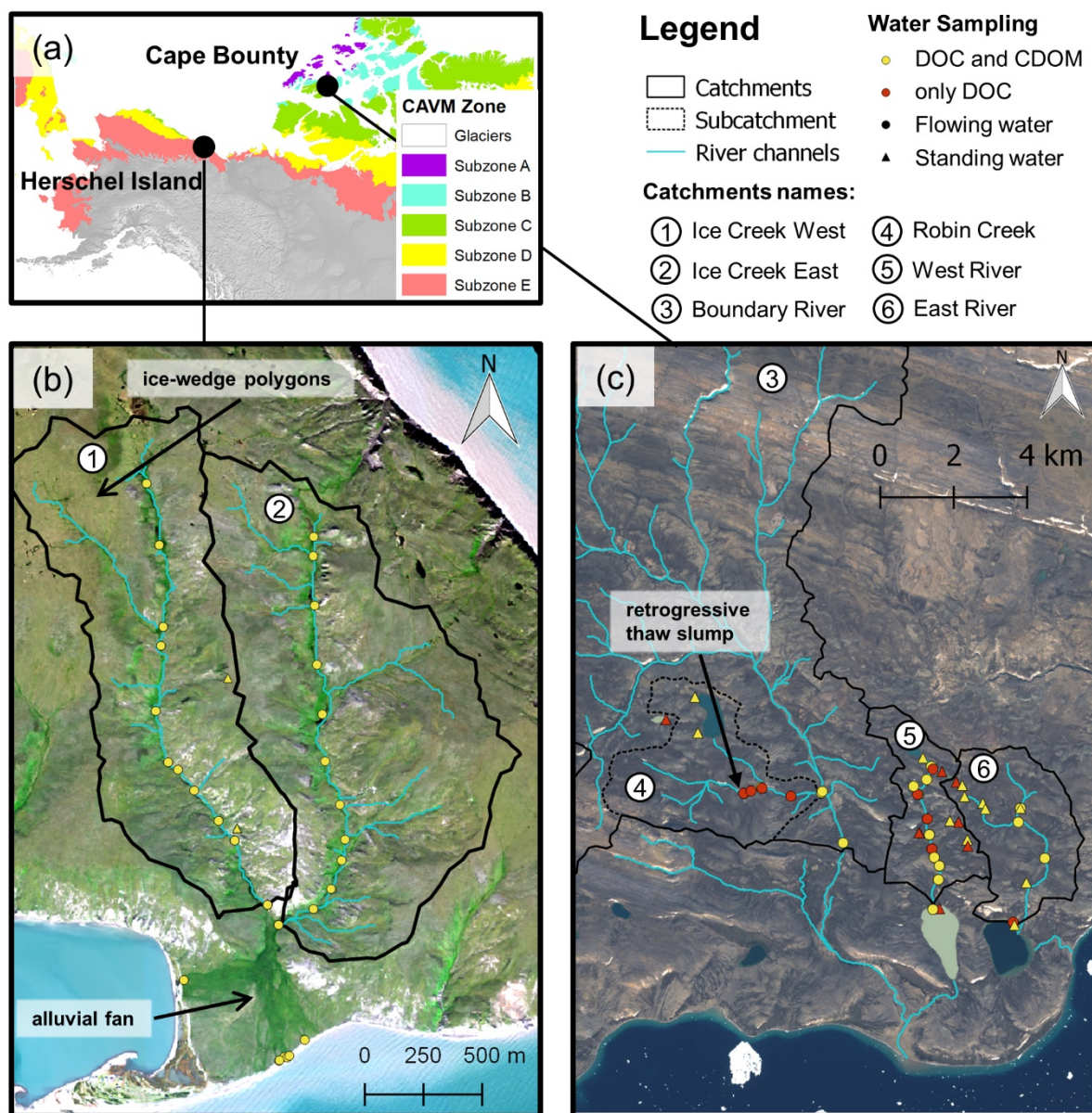
Figure 1. Maps of the study area showing (a) the location of Herschel Island and Cape Bounty in the Canadian Arctic including the
5 **CAVM bioclimatic zones (Walker & Raymond 2016), (b) the studied catchments Ice Creek West and Ice Creek East on Herschel Island and (c) the studied catchments Boundary River with its subcatchment Robin Creek (dashed watershed), West River and East River. The watershed names are indicated with numbers. Note that samples from flowing water (rivers and streams) are indicated by circles, whereas samples from standing water (ponds and lakes) are indicated by triangles. Yellow colors mark locations where DOC and CDOM measurements are available, while only DOC values are available at red locations. The background images are**
10 **true color mosaics (Herschel Island: WorldView-3 quasi-true color RGB composite, acquired on 8 August 2015; Cape Bounty: Sentinel-2 quasi-true color RGB composite, acquired on 7 August 2016).**
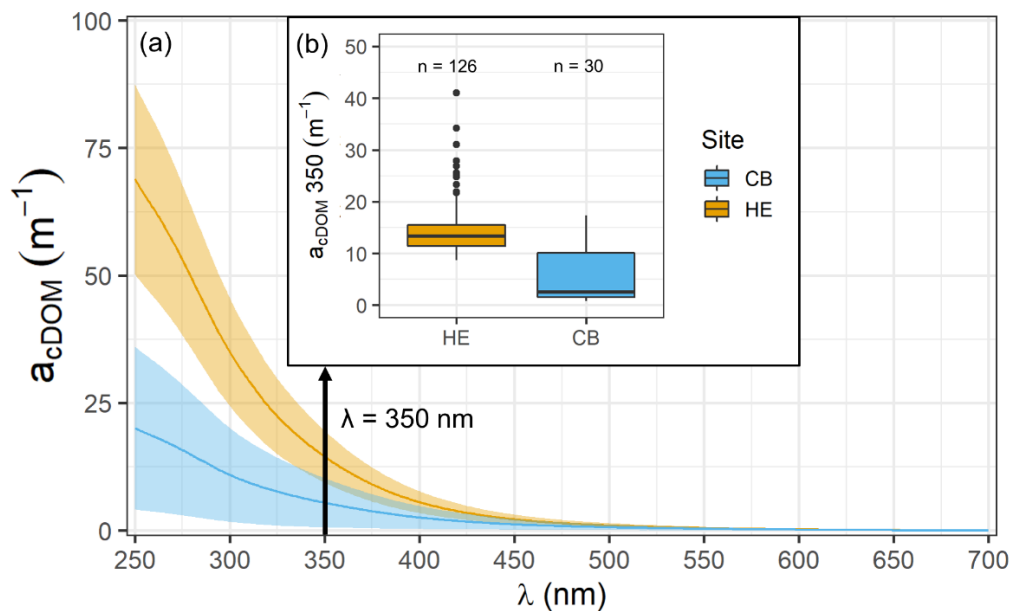
Figure 2. Absorption characteristics for the sites from Herschel Island (HE, in orange) and Cape Bounty (CB, in blue). (a) Average absorption (m⁻¹) for the wavelengths (λ) between 250 and 700 nm. The colored shaded areas represent the standard deviation from
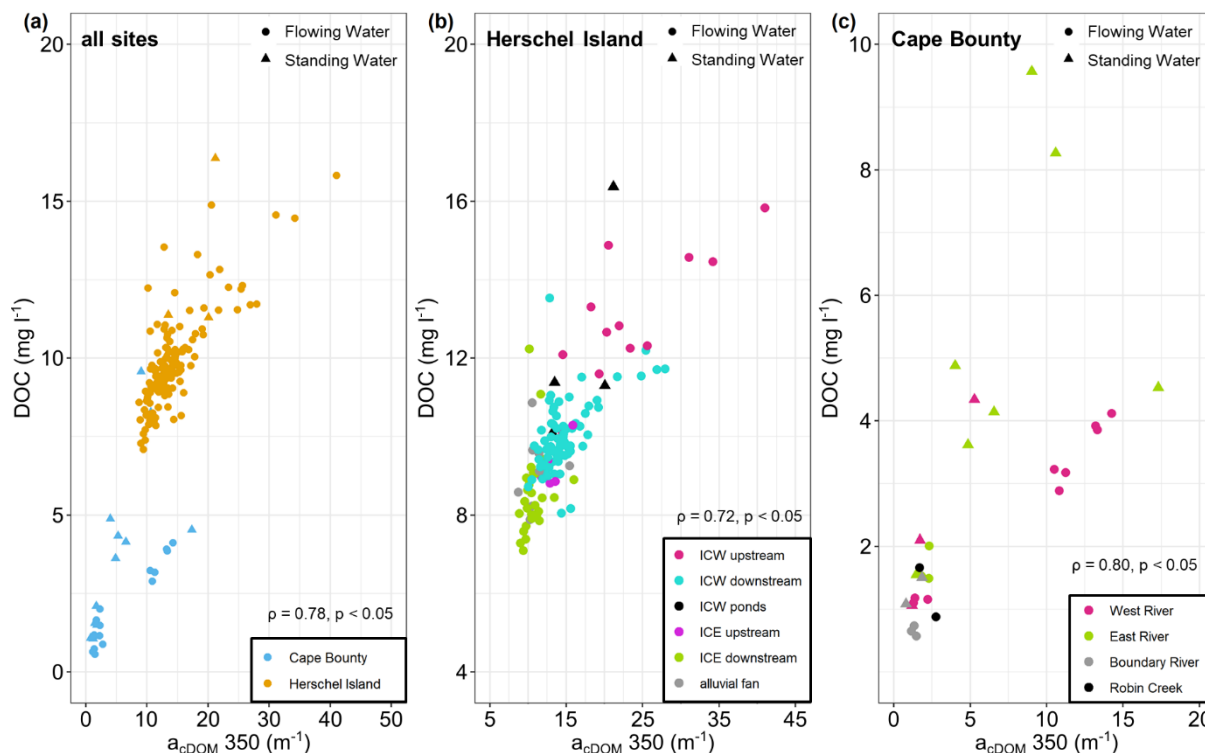5 **the mean (solid line). (b) boxplots of absorption at 350 nm for both sites.**

Figure 3. Absorption of cDOM at 350 nm (m⁻¹) versus DOC concentration (mg l⁻¹) for (a) all sites, (b) sites on Herschel Island and (c) sites at Cape Bounty. Note that flowing water is indicated by a circle while standing water such as lakes or ponds is indicated by a triangle.
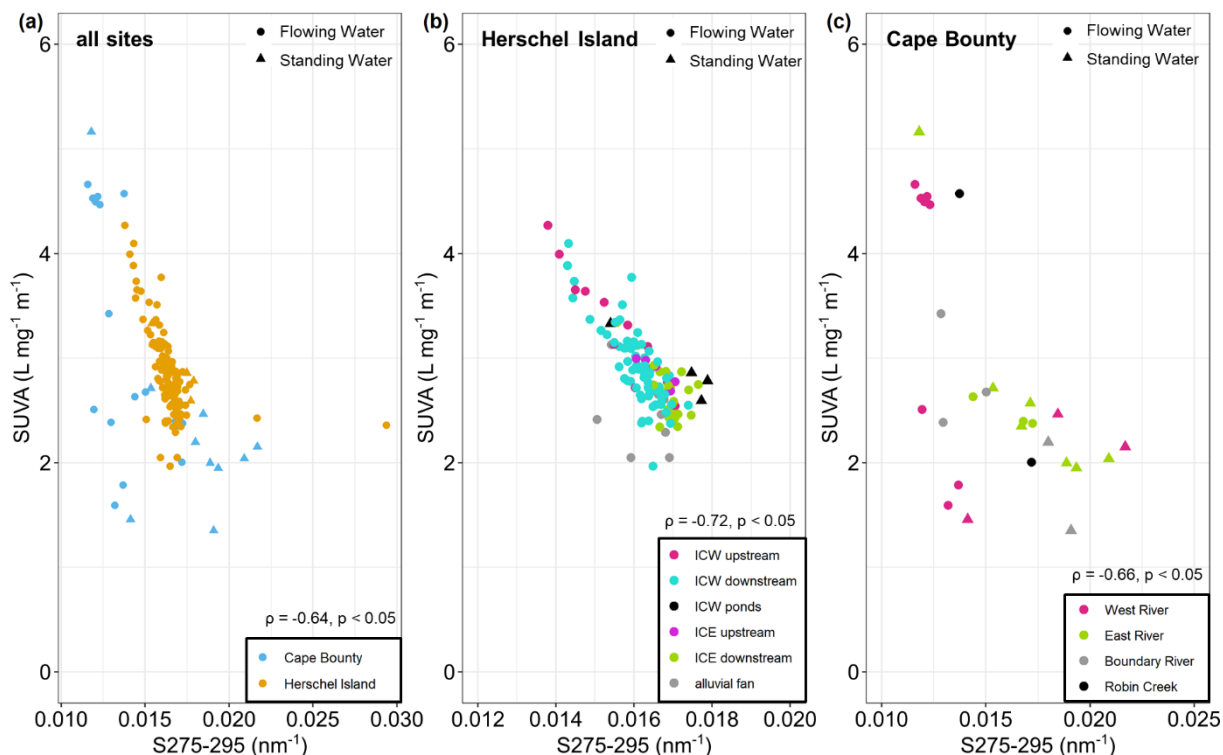
5

Figure 4. Slope of cDOM UV absorption 275-295 (nm⁻¹) versus SUVA (L mg⁻¹ m⁻¹) for (a) all sites, (b) sites on Herschel Island and (c) sites at Cape Bounty. Note that flowing water is indicated by a dot while standing water such as lakes or ponds is indicated by a triangle.
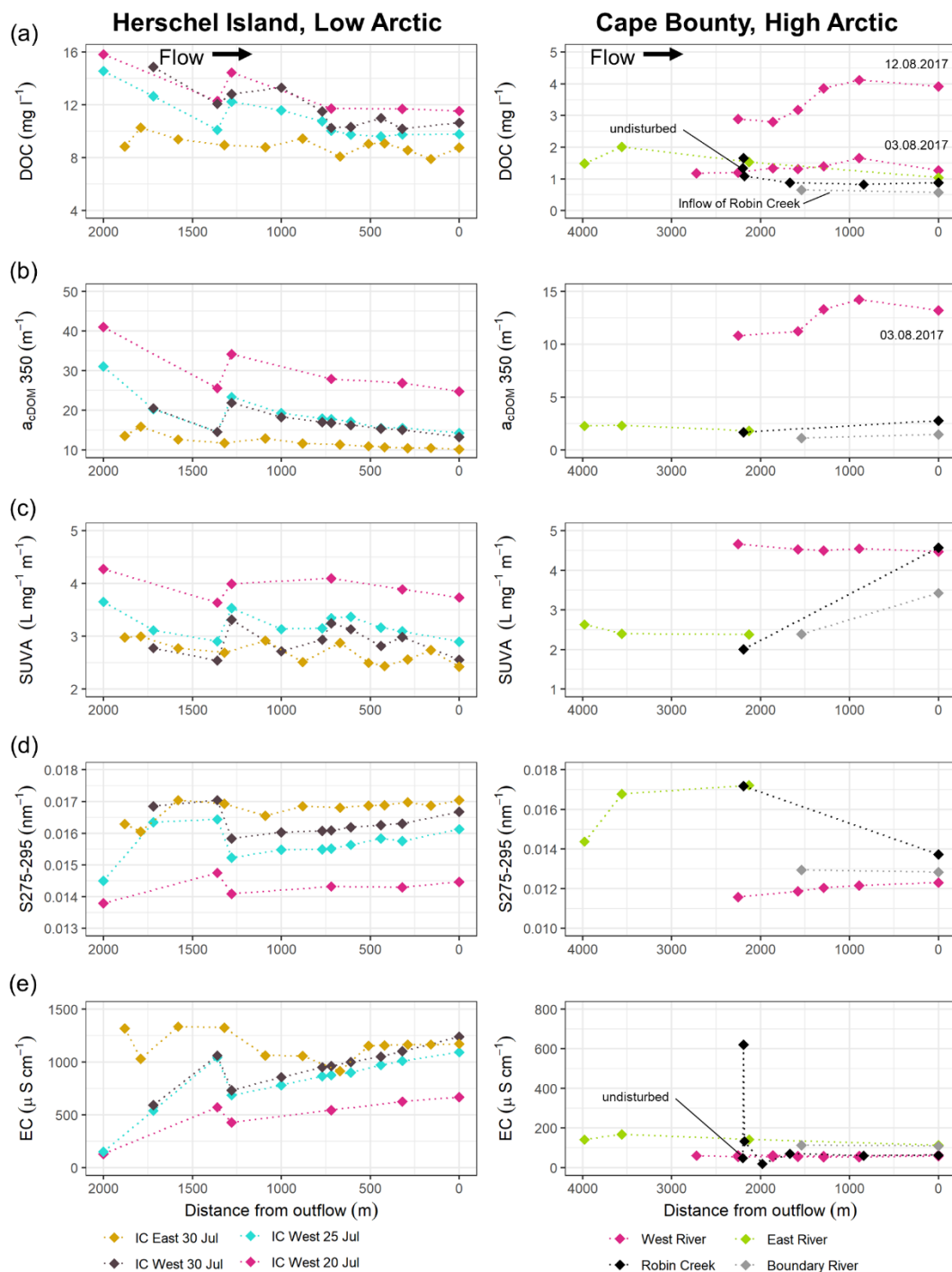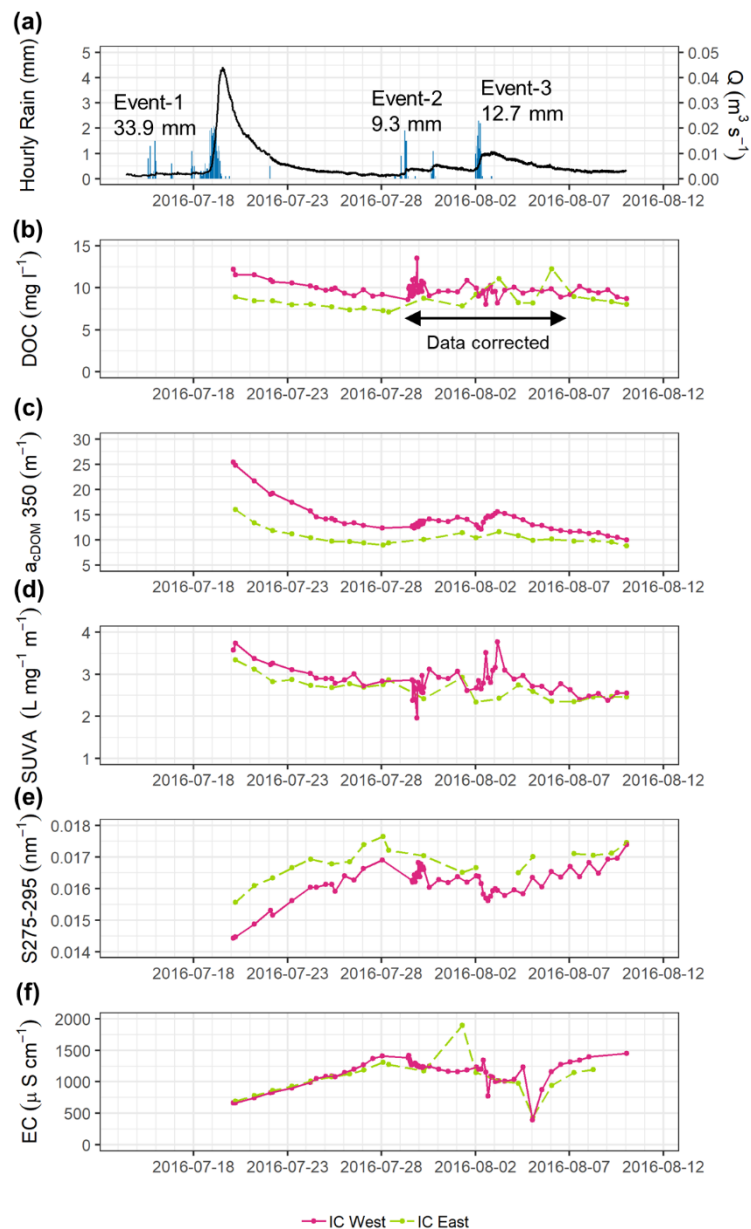
5

Figure 5. River transects showing values of (a) DOC (mg l^{-1}), (b) a$_{cDOM}$350, (c) SUVA (L mg^{-1} m^{-1}), (d) cDOM Slope S275-295 (nm^{-1}), (e) electrical conductivity for rivers on Herschel Island (left) and Cape Bounty (right). Note that IC West on Herschel Island was sampled at different dates as indicated in the legend.

Figure 6. Time series from Herschel Island showing (a) Discharge (m^3 s^{-1}) and hourly rainfall (mm) from Ice Creek West, (b) DOC concentration (mg l^{-1}), (c) $a_{CDOM}350$ (m^{-1}), (d) SUVA (L mg^{-1} m^{-1}) and (e) the S275-295 (nm^{-1}) over the summer season 2016 for Ice Creek West (magenta) and Ice Creek East (green) respectively. The label "data corrected" indicates the time period during which samples were frozen on site instead of being acidified immediately in the field.
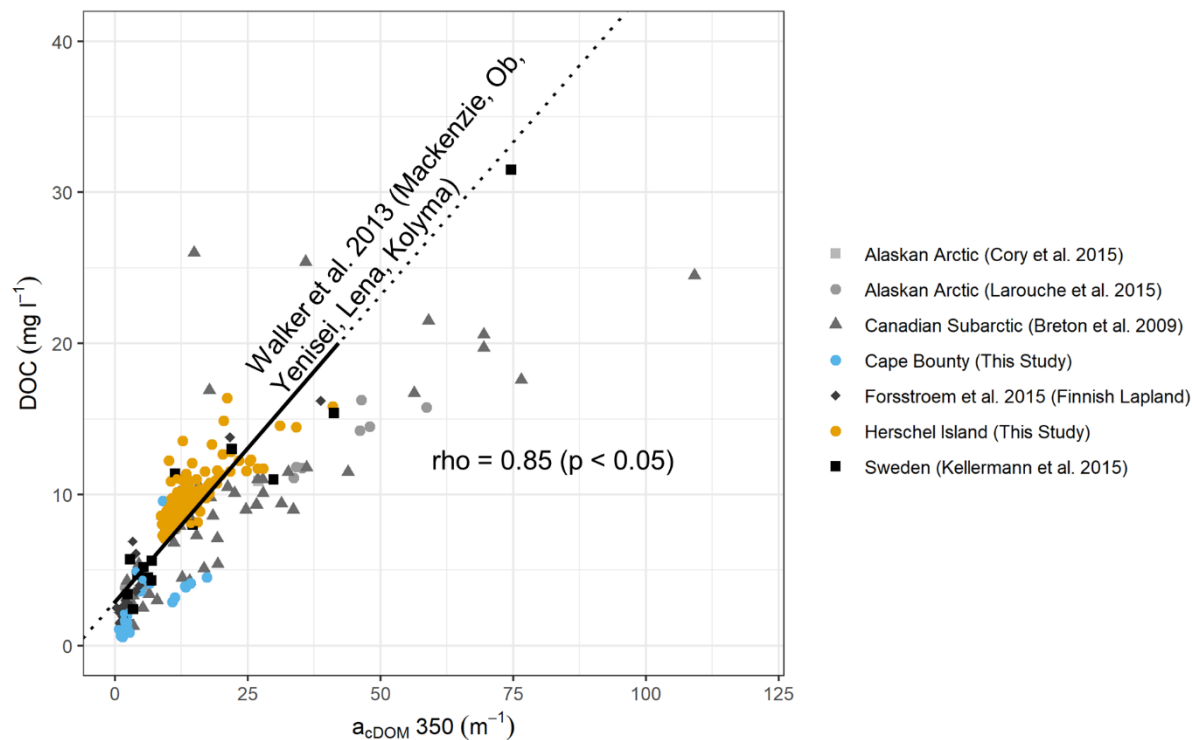
Figure 7. Relationship between $a_{cDOM}350$ (m^{-1}) and DOC concentration (mg l^{-1}) for our study sites (Herschel Island in orange and Cape Bounty in blue) and sites retrieved from the literature. The black lines represent the regression line established for the large Arctic rivers by Walker et al. (2013). The solid section marks the validity ranges for the relationship established, whereas the dotted line is the linear continuation.
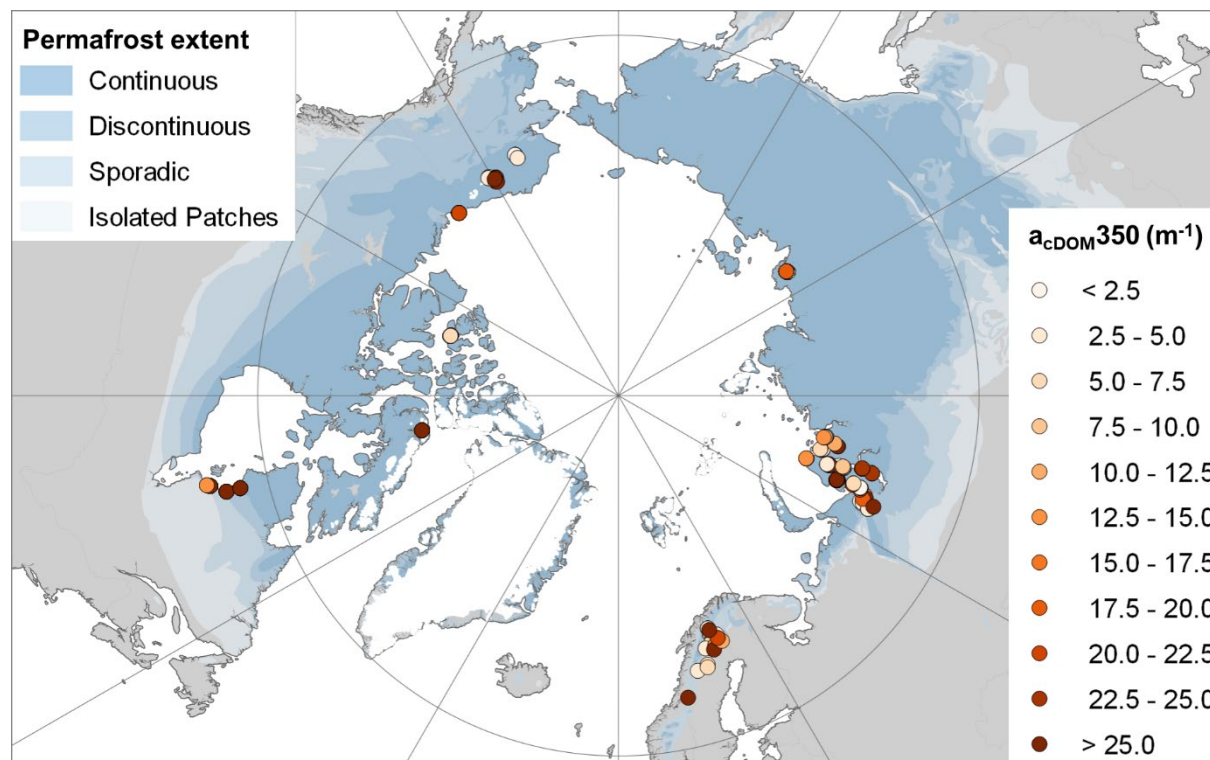
Figure 8. Values for a$_{cDOM}$350 across the Arctic region from this study and retrieved from the literature. The blue colour shows the permafrost extent (from continuous to isolated) and the color code of the points shows a$_{cDOM}$350 between < 2.5 m^{-1} and > 25 m^{-1}.

Tables

Table 1. Characteristics of studied watersheds on Herschel Island (Low Arctic) and Cape Bounty (High Arctic) showing catchment size (km^2), channel length (km), CAVM bioclimatic zone (CAVM, 2003), soil organic carbon content (SOCC) (Hugelius et al., 2013; Ramage et al., in review) and maximum catchment elevation above sea level (m).

Site	Catchment size (km^2)	Channel length (km)	Vegetation zone (CAVM)	Soil Organic Carbon content 0-30cm/0-100cm (kg m^2)	Maximum catchment elevation (m above sea level)
Herschel Island, Low Arctic					
Ice Creek West	1.4	2.2	Subzone D	11.4 / 26.4	88
Ice Creek East	1.6	1.9	Subzone D		95
Cape Bounty, High Arctic					
Boundary River	152.5	22.7	Subzone B/C		213
Robin Creek	14.8	5.1	Subzone B/C	3.0 / 10.2	151
West River	8.8	4.2	Subzone B/C		94
East River	12.4	5.2	Subzone B/C		103

5

Table 2. Descriptive statistics (mean ± standard deviation) of DOC (mg l^{-1}), SUVA$_{254}$ (L mg^{-1} m^{-1}), a$_{cDOM}$350 (m^{-1}), cDOM Slope S275-295 (nm^{-1}), SR, EC (μS cm^{-1}), pH and the number (n) of all samples/samples with cDOM absorption measurements. The statistics are given for specific rivers, samples from flowing waters, standing waters and all samples on Herschel Island and Cape Bounty respectively. The symbols ">" and "<" indicate significant inter-group differences (p < 0.05, p <0.01).

Site	EC μS cm^{-1}	pH	DOC mg l^{-1}	SUVA L mg^{-1} m^{-1}	a$_{cDOM}$350 m^{-1}	Slope 275-295 nm^{-1}	SR	n
Herschel Island, Low Arctic								
Ice Creek West	1050 ± 310	8.2 ± 0.2	10.4 ± 1.5	3.0 ± 0.4	16.1 ± 5.4	0.016 ± 0.001	0.83 ± 0.02	90/82
Ice Creek East	1030 ± 340	8.2 ± 0.2	8.7 ± 1.1	2.7 ± 0.2	11.1 ± 1.8	0.017 ± 0.002	0.90 ± 0.12	32/32
Alluvial fan	970 ± 170	7.8 ± 0.2	9.2 ± 0.9	2.5 ± 0.4	11.1 ± 1.9	0.016 ± 0.001	0.84 ± 0.02	8/8
Flowing Water (all)	1040 ± 310	8.2 ± 0.2	9.9 ± 1.5	2.9 ± 0.4	14.5 ± 5.1	0.016 ± 0.001	0.85 ± 0.07	130/122
Standing Water (all)	1440 ± 1300	8.3 ± 0.1	12.3 ± 2.8	2.9 ± 0.3	17.0 ± 4.2	0.017 ± 0.001	0.93 ± 0.06	4/4
All samples	1050 ± 370	8.2 ± 0.2	10.0 ± 1.6	2.9 ± 0.4	14.5 ± 5.1	0.016 ± 0.001	0.85 ± 0.07	134/126
Standing (S) vs. Flowing (F)	S ≈ F	S ≈ F	S > F	S ≈ F	S ≈ F	S ≈ F	S > F	n.a.
Cape Bounty, High Arctic								
Boundary River	110 ± 3	7.1 ± 0.0	0.7 ± 0.1	2.8 ± 0.5	1.3 ± 0.2	0.014 ± 0.001	1.13 ± 0.06	3/3
Robin Creek	145 ± 213	7.3 ±0.6	1.1 ± 0.3	3.3 ± 1.8	2.2 ± 0.8	0.015 ± 0.002	1.03 ± 0.12	7/2
West River	60 ± 17	6.9 ± 0.3	2.5 ± 1.7	3.6 ± 1.4	8.5 ± 5.2	0.012 ± 0.001	0.86 ± 0.10	19/8
East River	141 ± 22	7.3 ± 0.1	1.5 ± 0.4	2.5 ± 0.1	2.1 ± 0.3	0.016 ± 0.002	0.95 ± 0.06	4/3
Flowing Water (all)	92 ± 101	7.0 ± 0.4	1.9 ± 1.5	3.2 ± 1.2	5.5 ± 5.1	0.013 ± 0.002	0.94 ± 0.13	33/16
Standing Water (all)	210 ± 160	7.5 ± 0.6	3.4 ± 2.4	2.4 ± 1.0	5.4 ± 4.9	0.018 ± 0.003	1.14 ± 0.20	20/12
All samples	137 ± 136	7.2 ± 0.5	2.5 ± 2.0	2.8 ± 1.1	5.5 ± 4.9	0.015 ± 0.003	1.02 ± 0.19	53/28
Standing (S) vs. Flowing (F)	S > F	S > F	S > F	S < F	S ≈ F	S > F	S > F	n.a.
He_all vs. CB_all	HE > CB	HE > CB	HE > CB	HE > CB	HE > CB	HE > CB	HE > CB	n.a.

5

Table 3. Correlation matrix using the Spearman's rho correlation coefficient between latitude, DOC, $a_{cDOM}350$, soil organic carbon content in 0-30 cm and 0-100 cm depth (Hugelius et al. 2014). Significance levels of $p < 0.05$ and $\underline{p \leq 0.01}$ are indicated.

	Latitude	$a_{cDOM}350$	DOC	SOCC 0-30cm	SOCC 0-100cm
Latitude	1.00	**<u>-0.22</u>**	**-0.13**	**<u>-0.19</u>**	**<u>-0.26</u>**
$a_{cDOM}350$		1.00	**<u>0.85</u>**	**<u>0.26</u>**	**<u>0.34</u>**
DOC			1.00	**<u>0.53</u>**	**<u>0.51</u>**
SOCC 30cm				1.00	**<u>0.71</u>**
SOCC 100cm					1.00

5